Development 127, 4655-4668 (2000)
Printed in Great Britain © The Company of Biologists Limited 2000
DEV9721

Establishment of left/right asymmetry in neuroblast migration by UNC-40/DCC, UNC-73/Trio and DPY-19 proteins in *C. elegans*

Lee Honigberg* and Cynthia Kenyon‡

Program in Neuroscience and Department of Biochemistry and Biophysics, University of California, San Francisco, CA 94143-0448, USA

*Present address: Axys Pharmaceuticals, 180 Kimball Way, South San Francisco, CA 94010, USA

‡Author for correspondence (e-mail: ckenyon@biochem.ucsf.edu)

Accepted 27 July; published on WWW 9 October 2000

SUMMARY

The bilateral *C. elegans* neuroblasts QL and QR are born in the same anterior/posterior (A/P) position, but polarize and migrate left/right asymmetrically: QL migrates toward the posterior and QR migrates toward the anterior. After their migrations, QL but not QR switches on the *Hox* gene *mab-5*. We find that the UNC-40/netrin receptor and a novel transmembrane protein DPY-19 are required to orient these cells correctly. In *unc-40* or *dpy-19* mutants, the Q cells polarize randomly; in fact, an individual Q cell polarizes in multiple directions over time. In addition, either cell can express MAB-5. Both UNC-40 and DPY-19, as well as the Trio/GTPase exchange factor homolog UNC-73, are required for full polarization and migration. Thus, these proteins appear to participate in a signaling system that orients and polarizes these migrating cells in a left/right asymmetrical fashion during development. The *C. elegans* netrin UNC-6, which guides many cells and axons along the dorsoventral axis, is not involved in Q cell polarization, suggesting that a different netrin-like ligand serves to polarize these cells along the anteroposterior axis.

Key words: *C. elegans*, Neuroblasts, UNC-40, DPY-19, UNC-73, Netrin, Cell migration, Left/right asymmetry

INTRODUCTION

The left/right (L/R) asymmetry of *Caenorhabditis elegans* is established at the six-cell stage by cell-cell interactions and is manifest as subsequent L/R differences in many tissues in the developing animal (Hutter and Schnabel, 1995; Wood, 1991). One particularly intricate asymmetry involves the behavior of the Q neuroblasts. QL, on the left side of the animal, migrates toward the posterior, whereas QR, on the right side, migrates toward the anterior (Fig. 1A). After their migrations, QL starts to express the Antennapedia-like *Hox* gene *mab-5* (Salser and Kenyon, 1991). *mab-5*, which specifies many cell fates in the posterior body region (Kenyon, 1986), acts as a switch to control the direction of migration in the Q neuroblast descendants: when *mab-5* is ON the Q descendants migrate to remain in the posterior and when *mab-5* is OFF the Q descendants migrate anteriorly (Fig. 1B). In *mab-5*(–) animals, QL itself migrates normally toward the posterior, but the QL descendants then migrate anteriorly (Chalfie et al., 1983). MAB-5 expression is not only necessary, but also sufficient for the posterior pattern of migration in the Q descendants. Ectopic expression of MAB-5 in the QR descendants can cause them to migrate posteriorly (Salser and Kenyon, 1991). Mosaic analysis and laser induced single-cell delivery of heat-shock-*mab-5* have shown that *mab-5* acts in the Q descendants to determine their direction of migration (Harris et al., 1996; Kenyon, 1986).

The L/R asymmetrical expression of MAB-5 is established by a Wnt signaling pathway that includes EGL-20/Wnt, LIN-17/Frizzled and BAR-1/beta-catenin (Eisenmann et al., 1998; Maloof et al., 1999; Sawa et al., 1996). EGL-20/Wnt, which activates MAB-5 expression in QL, is expressed in several posterior cells near the Q neuroblasts. However, the asymmetry of MAB-5 expression in the Q cells does not appear to result from left-right or anterior-posterior differences in EGL-20 expression levels. If EGL-20 is mis-expressed in anterior cells (using the pharyngeal *myo-2* promoter), it still only activates *mab-5* in QL. EGL-20 dose-response experiments indicate that QL is more sensitive to EGL-20 than is QR. This suggests that QL but not QR expresses MAB-5 during normal development because the endogenous level of EGL-20 is sufficient to activate *mab-5* in QL but not in QR (Whangbo and Kenyon, 1999).

Prior to the activation of *mab-5*, the earliest asymmetry in the Q cells is their migration in opposite directions (Fig. 1A). This asymmetry does not require *mab-5* or *egl-20* (Harris et al., 1996; Salser and Kenyon, 1991). To understand how the first asymmetry in the Q cells is generated and how it is linked to their differential sensitivity to Wnt signaling, we have identified mutants that disrupt the migration of QL and QR.

We find that three genes are required for the migration of QL and QR: *unc-40*, *dpy-19* and *unc-73*. *unc-40* encodes a receptor that acts in an evolutionarily conserved system for guiding dorsal-ventral (D/V) cell and axon migrations. In *C.*

elegans, *unc-40* is required for the growth of many cells toward the ventral midline. These midline cells express UNC-6/netrin and mutations in *unc-6* prevent normal ventral as well as dorsal guidance. (A second receptor, UNC-5, allows cells to migrate dorsally, away from UNC-6.) *Drosophila* and mouse mutants lacking *unc-6* and *unc-40* homologs also cause incorrect D/V guidance, demonstrating that the function of these proteins is widely conserved. Purified netrin has been shown to act as a chemoattractant for ventrally directed commissural axons in the spinal cord (Kennedy et al., 1994; Serafini et al., 1994) and as a chemorepellent for dorsally directed trochlear motoneurons (Colamarino and Tessier-Lavigne, 1995). The vertebrate UNC-40 homolog, DCC, binds UNC-6/netrin and anti-DCC antibodies block the chemoattraction by netrin (Keino et al., 1996). Thus UNC-6 functions directly as a ligand for the UNC-40 receptor.

In addition to its role in D/V guidance, *unc-40* in *C. elegans* is also required for a small number of non-D/V migrations that do not appear to require *unc-6* (Hedgecock et al., 1990). In *unc-40* mutants, the descendants of the Q cells are often found in the wrong location. By analyzing these mutants in more detail we find that *unc-40* mutations affect a specific, very early, step in these migrations: the polarization and migrations of QL and QR. Mutations in *unc-40* prevent the Q neuroblasts from migrating and cause them instead to polarize in random directions. Subsequently, the Q cells mis-express MAB-5, which then causes their descendants to migrate incorrectly. Neither of these defects is present in *unc-6*/netrin mutants.

dpy-19 was originally identified as one of a large set of genes that, when mutated, cause animals to be short (dumpy) (Brenner, 1974). We found that mutations in *dpy-19* cause the same defects in the Q cells as seen in *unc-40* mutants: the Q cells polarize incorrectly and their descendants mis-express MAB-5. Unlike *unc-40*, *dpy-19* does not function in D/V guidance, but functions specifically to orient the Q cells along the A/P axis. *dpy-19* is homologous to a human brain-expressed cDNA and encodes a novel transmembrane protein. These results suggest that *dpy-19* may define a new component of a conserved UNC-40/DCC dependent guidance system.

The UNC-73 protein is required for directed growth and guidance of many cells and axons along both the A/P and D/V body axes (Forrester and Garriga, 1997; Hedgecock et al., 1987; McIntire et al., 1992; Way et al., 1992). The sequence of UNC-73 is similar to the evolutionarily conserved Trio protein (Steven et al., 1998). Trio contains multiple domains including spectrin-like repeats, two Dbl/pleckstrin-homology guanine-nucleotide-exchange-factor (GEF) domains, and an SH3-like domain. We find that mutations in *unc-73* prevent the migrations of QL and QR, but, in contrast to *dpy-19* and *unc-40*, only mildly disrupt the direction of the Q polarizations and the expression of MAB-5 in the Q descendants.

Our findings suggest that a system analogous to the netrin-based D/V system is used to create L/R asymmetry in the Q cell migrations. This system does not require the known *C. elegans* netrin, UNC-6, and so may involve a different netrin-like ligand. We propose that L/R asymmetry arises either by the L/R asymmetrical placement of this UNC-40 ligand or by the L/R asymmetrical expression of a receptor in the Q cells, which allows them to respond differentially to signals that are present on both sides of the animal. In either case, these signals would lead to changes in the cytoskeleton by acting through UNC-73 and its GTPase targets to allow the Q cells to polarize in opposite directions and subsequently to express MAB-5 in a L/R asymmetrical pattern.

MATERIALS AND METHODS

General methods and genetics

C. elegans strains were maintained and genetically manipulated as described (Sulston and Hodgkin, 1988). All alleles of *unc-40*, *dpy-19* and *unc-73* examined were temperature sensitive for their polarization and MAB-5 expression phenotypes. The phenotypes at 15°C, 20°C and 25°C in these mutants were qualitatively similar, but more penetrant at higher temperatures. Because *unc-40(e1430)* and *dpy-19(n1348)* are likely to be null alleles, the temperature dependence presumably reflects the temperature sensitivity of some underlying process. Wild-type worms were not temperature sensitive for any of the phenotypes examined here. All data were collected at 20°C, with the following exceptions: *unc-40(e271)* and *unc-40(e1430)* were scored at 25°C in Figs 3, 7 and 8 to illustrate their phenotypes more clearly; *dpy-19(n1347n1348)* was scored at 15°C in Figs 3 and 8 because the strain was extremely unhealthy at 20°C. The time at which the Q cell shape was scored in animals grown at 15°C or 25°C was adjusted appropriately to compensate for different developmental rates at these temperatures.

Because *unc-73(gm33)* animals have few or zero progeny, *unc-73(gm33)* strains were maintained using sDp2, a free duplication that contains *unc-73(+)*. *unc-73(gm33)* progeny from *unc-73(gm33);sDp2* worms were identified by the shortened HSN (Hermaphrodite Specific Neuron) migration phenotype of *unc-73* mutants (Desai et al., 1988) and then scored for Q cell shape (in Fig. 3) or MAB-5 staining (in Fig. 6).

Microscopy and scoring of cell shapes and positions

Animals were staged by washing the hatched worms from a plate of eggs with M9 at 30 minute intervals. These ‘hatchoffs’ were filtered through 13 μm Nytex mesh to remove eggs accidentally carried up in the wash and then spotted on seeded plates.

To measure the extent of the QL and QR migrations, animals from a hatchoff were mounted on 2 mM sodium azide pads. Measurements before the Q migration were taken from 0 to 30 minutes after hatchoff and measurements after the Q migration were taken from 2.75 to 3.25 hours after hatchoff. Straight, nonmoving worms with undivided Q cells were selected and Nomarski video images of the left and right sides were acquired using a Scion LG framegrabber for later analysis. Using NIH Image, the center of the nucleoli of QL and QR were marked, and the straight-line distance between these two points was calculated. The distances of QL and QR from a fixed point on the animal, the posterior end of the intestine, were also measured. From these data, we found that all mutants described here affected the migration of QL and QR equally, and so we have used the QL-QR distance as our single metric.

To measure the degree of polarization, animals were mounted on 2% agarose pads starting at 2 hours after hatchoff collection and scored for the next 30 minutes. Based on observations of many animals over time, we know that the Q cells extend from their dorsal edge, while the ventral edge remains stationary. Thus, in all cases we judged the direction of polarization by observing the dorsal, leading edge of the cell. For Fig. 3, the distance reached by the Q cells was scored relative to neighboring V cells in the following categories: –, Q was round or irregularly shaped; >, Q pointed toward V5, but did not reach as far as the A/P midpoint of V5; >>, the most posterior tip of Q extended to the midpoint of V5; >>>, the most posterior tip of Q extended past the midpoint of V5. <, << and <<< are defined similarly for the polarization toward the anterior, except relative to a point which is one-third the distance from the posterior to anterior

edge of V4. (The cell P7,8 is positioned between Q and V4, so polarization toward the anterior does not reach as far relative to V4.) In separate experiments to photograph cell shapes, animals were mounted on agarose pads containing 2 mM sodium azide. Long-term exposure to sodium azide sometimes caused retraction of cell outlines, so animals were examined within 15 minutes of mounting. Images were collected using a BioRad MRC-600 confocal microscope, and then later rotated and contrast-enhanced using Adobe Photoshop.

For Fig. 4, in which the cell shape was followed over time in individual animals, 0-30-minute-old worms were mounted on 2% agarose pads. Every 15 or 20 minutes, the Q cells were brought into focus using Nomarski optics, and then exposed for 100-200 mseconds using a standard fluoroscein filter set and a Uniblitz shutter (Vincent Associates) connected to an Apple Macintosh computer. Custom macros in NIH Image were used to open and close the shutter, and to control image accumulation on a Photometrics Imagepoint CCD camera. Images were stored on laser videodisc for later analysis. Multiple fluorescence exposures in a short period caused the worms to move rapidly away from the illumination and also caused significant photobleaching; thus, only one snapshot per timepoint was possible.

The final position of the Q descendants was determined in late L1 larvae using standard Nomarski optics. QL.paa and QL.pap (also known as PVM and SDQL) were scored on the left side and QR.paa and QR.pap (also known as AVM and SDQR) were scored on the right side. The QL.ap and QR.ap cells migrate into body regions with many other neurons, and therefore cannot be scored reliably. Cells were positioned relative to the epidermal cells V1-V6, each of which have divided once at the end of L1. We were unable to score the final position of the Q descendants in the stronger *unc-73* allele, *gm33* because these animals were unhealthy and had disorganized epidermal cells.

HSN, CAN, M and ALM cell positions were scored in 0-3-hour-old animals, relative to the V and P epidermal cells. The following positions were defined as wild-type: HSN, between P5,6 and V5; CAN, between V3 and V4; M, between P7,8 and V5; and ALM, between V2 and V3. DTC and Linker cell migrations were scored at 36 hours after hatching and compared with wild type (Sulston and Horvitz, 1977).

MAB-5 antibody staining was performed as described in Salser et al. (1993).

Cloning *dpy-19*

The strain MT3128 *dpy-19(n1347)* contains a Tc1 transposon insertion in *dpy-19* (M. Finney, personal communication). DNA adjacent to all the Tc1 insertions in this strain was amplified by PCR and this mix of amplified fragments was then probed against a Southern blot of cosmids in the *dpy-19* region (S. Collums and R. Plasterk, personal communication). This led to the tentative mapping of *dpy-19* to the predicted gene F22B7.10, which had been identified by the *C. elegans* genome sequencing project (Sulston et al., 1992). We used RT-PCR and 3′ RACE (Frohman, 1993) to amplify cDNAs containing sequences from F22B7.10 and were able to define a single SL1-spliced transcript (Fig. 5). The sequence of this transcript matched the computer-predicted splice sites in F22B7.10, with the exception of the first exon and intron. The corrected splice form has been submitted to Genbank and ACeDB.

For northern analysis, RNA from N2 (wild type) and *dpy-19(n1347n1348)* was prepared using Trizol (Gibco-BRL) according to the protocol of R. Burdine and M. Stern (personal communication). 20 μg of total RNA/lane was blotted using standard techniques (Sambrook et al., 1989) and the blot was probed with digoxigenin-labeled RNA, according to manufacturer's instructions (Genius Kit, Boerhinger). The *dpy-19* antisense probe was generated by in vitro transcription, using an RT-PCR product spanning exons 6-9 as a template.

We rescued the Dpy and Q phenotypes of *dpy-19(mu78)* by injecting the cosmid C27E4 (which overlaps F22B7) at 12.5 μg/ml using standard techniques (Mello et al., 1991). We then narrowed the rescuing activity to a 10 kb *Bgl*II fragment (injected at 12.5 μg/ml) that contains 1.5 kb upstream and 1.0 kb downstream of the *dpy-19* gene.

To identify the mutations in *dpy-19* alleles, genomic sequences covering the *dpy-19* coding region were amplified from the alleles *mu78*, *mu79*, *e1259* and *e1314*. DNA was either amplified with Taq (Roche) and sequenced directly, or amplified with Pwo hi-fidelity polymerase (Boerhinger), purified using Geneclean (Bio101), treated with Taq and dATP to add A overhangs, and then subcloned into pGEM-T vector (Promega) for sequencing. In all cases, mutations were confirmed by sequencing from a second PCR amplification. We confirmed that *dpy-19(n1347)* contained a Tc1 insertion in the *dpy-19* gene by PCR with *dpy-19*- and Tc1-specific primers. The approximate endpoints of the deletion in *n1347n1348* were determined by Southern analysis.

dpy-19 suppressor screen

unc-36(e251) dpy-19(e1259) animals were mutagenized with 25 mM EMS (ethylmethanesulfonate) as described in (Brenner, 1974). 34 pools of approx. 1000 F_1 animals each were grown at 20°C and allowed to lay eggs. L1 hatchoffs of approx. 10 000 F_2 animals/pool were collected and placed at 25°C. Suppressors were identified as fertile adult animals 3 days later, and maintained at 25°C to confirm suppression of the *dpy-19(e1259)* phenotype. We identified 13 confirmed suppressors, of which eight were known to be independent. All eight independent suppressors partially suppressed the Dpy and Q cell migration phenotypes caused by *dpy-19(e1259)*. To test for linkage, we crossed each of the eight suppressed strains to wild type. The appearance of UncDpy F_2 progeny would indicate an unlinked suppressor, but all eight suppressors appeared to be tightly linked to *dpy-19*. We tested four of the suppressors in complementation tests with *dpy-19(mu78)*. In all cases, *unc-36(e251) dpy-19(e1259) sup(?)/dpy-19(mu78)* animals were SemiDpy, implying that the suppressors were either intragenic revertants to near-wild-type levels of *dpy-19* activity or semidominant extragenic mutations. We sequenced the *dpy-19*-coding region in two of the suppressors (as described above for the sequencing of *dpy-19* alleles) and identified the intragenic mutations shown in Fig. 5A.

GFP fusion constructs

MIG-2::GFP

The rescuing, N-terminal tagged MIG-2::GFP fusion construct described in Zipkin et al. (1997) was co-injected with the cosmid *C14G10 [unc-31(+)]* into *unc-31(e169); him-5(e1490)* worms using standard techniques (Mello et al., 1991). We selected an extrachromosomal array carrying line and integrated the array using 3600 R of gamma-irradiation at 300 R/min. Of 10 integrated lines, we chose the one with highest MIG-2::GFP expression levels and outcrossed it three times to *unc-31(e169); him-5(e1490)*, selecting at each generation for animals with high levels of MIG-2::GFP expression. The outcrossed strain, *unc-31(e169); him-5(e1490); muIs28[mig-2::GFP+unc-31(+)]*, had wild-type Q descendant final positions (*n*=100). *muIs28* was then crossed into *dpy-19*, *unc-40*, and *unc-73* mutants. We found that *muIs28* partially suppressed *unc-40* and *unc-73* mutations. At 20°C, *unc-40(e271)* had 18% QL descendants anterior (*n*=50) while *unc-40(e271);muIs28* had 8% QL descendants anterior (*n*=50). *unc-73(e936)* had 4% QL descendants anterior (*n*=50) while *unc-73(e936);muIs28* had 0% QL descendants anterior (*n*=200). *unc-73(e936);muIs28* animals also appeared less uncoordinated than *unc-73(e936)* alone, but *muIs28* did not suppress the shortened HSN and QR descendant migration phenotypes of *unc-73(e936)*. Because we were concerned that *muIs28* could qualitatively change the Q cell shape phenotype in *unc-73* mutants, we used UNC-73::GFP to visualize the Q cells in all *unc-73* mutant strains.

UNC-73::GFP

The non-rescuing *evIn80[unc-73::GFP + rol-6D]* fusion (described

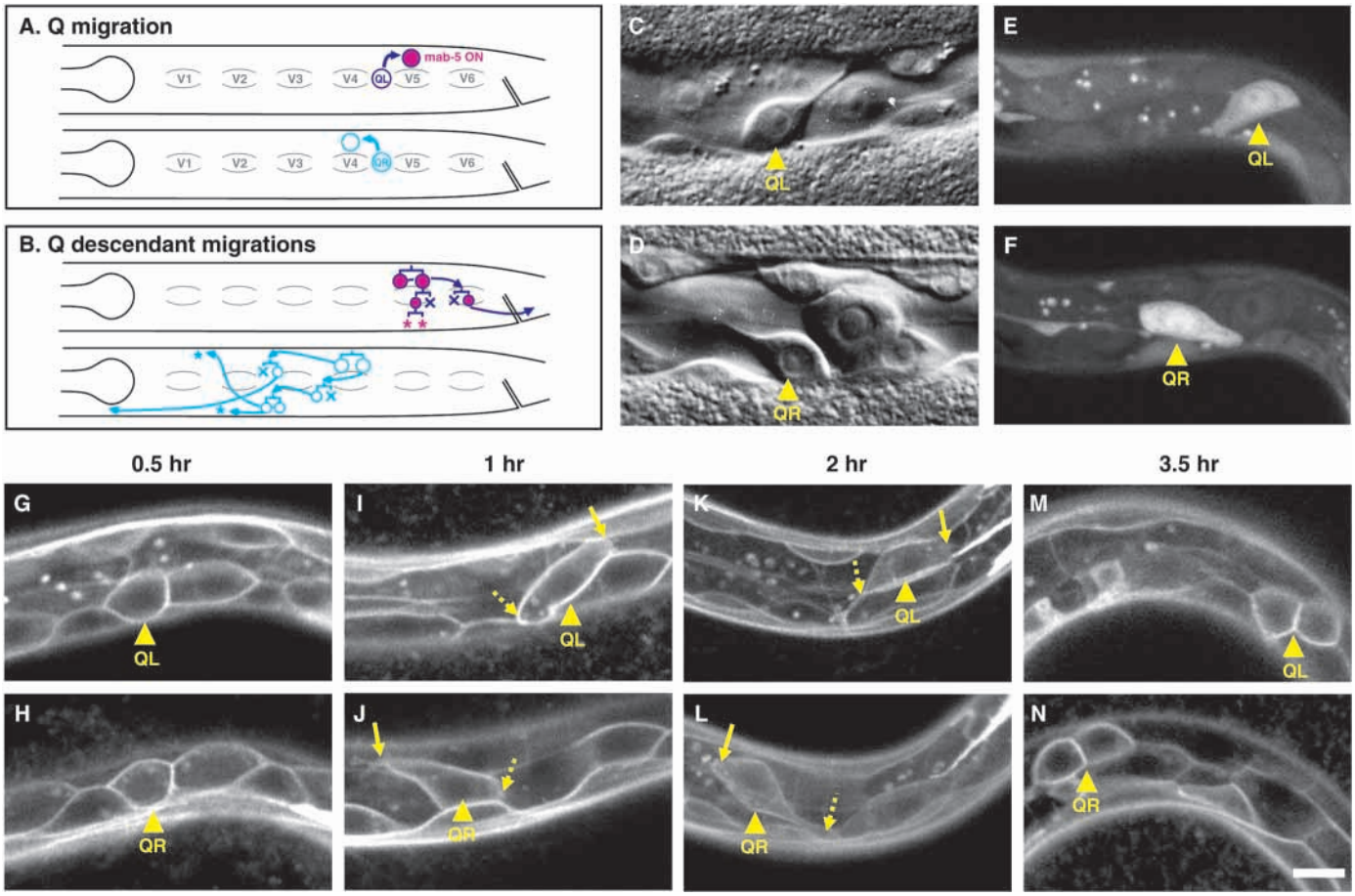

Fig. 1. Wild-type Q cell polarization and migration. (A) Schematic showing the migration of QL towards the posterior and QR towards the anterior. The epidermal cells V1-V6 are shown as landmarks. MAB-5 expression (shown in pink) begins in QL after its migration. (B) Pattern of divisions and further migrations of the Q descendants. X indicates cell deaths. *, the stopping points of the Q.paa and Q.pap cells; these are scored to determine the final position of the Q descendants. (C,D) QL and QR polarization in opposite directions visualized using *clr-1(e1745ts)* Animals were shifted from 20°C to 25°C at 60 minutes after hatching (to elicit Clear phenotype) and viewed 60 minutes later using Nomarski optics. (E,F) UNC-73::GFP expression on the left and right side of the worm at 1 hour after hatching. (G-N) MIG-2::GFP expression showing typical QL and QR cell shapes from 30 minutes after hatching (G,H) until the Q cells divide (M,N) at approx. 3.5 hours after hatching. Each time point shows left and right sides of the same animal. Arrowheads indicate QL on the left and QR on the right. The broken arrow marks the ventral trailing edge of the Q cells and the unbroken arrow marks the dorsal leading edge of cell. Scale bar: 5 μm. Anterior is towards the left, dorsal is upwards in all figures.

in Steven et al., 1998) was crossed into *unc-73* mutants using standard techniques. *unc-73(e936);evIn80* had 6% QL descendants anterior (*n*=50), similar to *unc-73(e936)* alone. We did not use UNC-73::GFP for all cell shape assays because it was not as reliably expressed in the Q cells as MIG-2::GFP and because UNC-73::GFP expression in the intestine often caused high background fluorescence.

UNC-40::GFP

evEx66[unc-40::GFP + rol-6D] is described in Chan et al. (1996).

DPY-19::GFP

Starting from genomic cosmid clones, we assembled a plasmid containing 4.4 kb of upstream sequence, the entire *dpy-19*-coding sequence (with introns) and 1.0 kb of downstream sequence. Because we did not know the membrane topology of DPY-19, we generated two different GFP-tagged fusions. For the N-terminal GFP-tagged construct, we used site-directed mutagenesis (Tomic et al., 1990) to insert a unique *Bam*HI site after the second codon of *dpy-19* and inserted F64L S65T GFP with 3 introns (from pPD114.35). For the C-terminal GFP-tagged construct, we used site-directed mutagenesis to make a silent change that introduced a *Bgl*II restriction site at the 3rd from last codon of *dpy-19*. We then inserted the coding sequence for S65T GFP with 3 introns (from pPD95.85). These constructs were injected at 100 μg/ml with *C14G10(unc-31(+))* at 30μg/ml to generate multiple transgenic strains. Both GFP-tagged fusions showed similar patterns of expression and fully rescued the Dumpy phenotype. The C-terminal fusion was tested for rescue of the Q cell migration defect. All worms carrying the array had QL.pax final positions posterior to V4.a, indicating complete rescue. For the transcriptional fusion, we inserted 4.4 kb of upstream sequence into a vector containing NLS::GFP::*lacZ* coding sequences and the *unc-54* 3′UTR (derived from pPD96.04). This fusion was injected at 100 μg/ml with *C14G10(unc-31(+))* at 30 μg/ml into *unc-31(e169)*. All pPD vectors were provided by A. Fire.

RESULTS

Overview of the Q neuroblast migrations in wild type

Shortly before the worm hatches, QL and QR are born as the anterior daughters of the Q/V5 precursor cells, which are

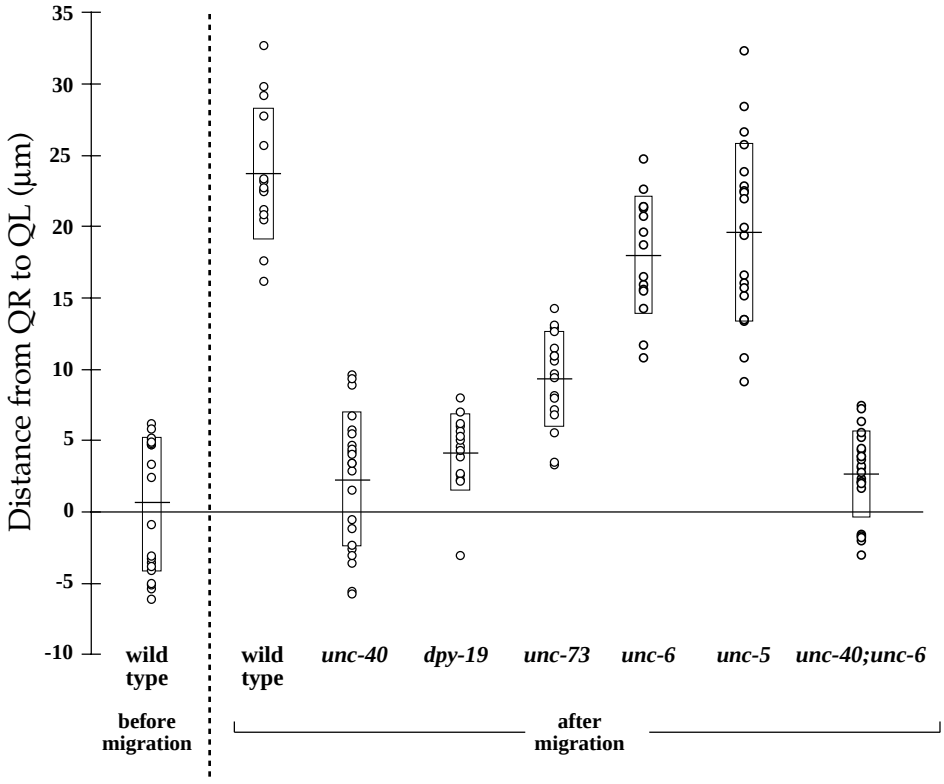

Fig. 2. Extent of the Q cell migrations. Each circle represents the straight-line distance along the A/P axis between the centers of the QL and QR nucleoli in an individual animal. Negative values indicate that the nucleolus of QR was more anterior than that of QL. Horizontal bars and boxes show mean and standard deviation, respectively. Alleles used: *unc-40(e271)*, *dpy-19(mu78)*, *unc-73(e936)*, *unc-6(ev400)* and *unc-5(e53)*. In all mutants, the Q cells divided between 3.5 and 4.0 hours after hatching, the same time as in wild type. *unc-40*, *dpy-19* and *unc-73* differ from wild type ($P<0.0001$); *unc-5* and *unc-6* differ from *unc-40* ($P<0.0001$); *unc-40;unc-6* does not differ from *unc-40* ($P>0.75$) (all P values from Bonferroni t test). *unc-6(ev400)* animals are variably small or mis-shapen, which may contribute to the decreased separation of the Q cells in *unc-6(ev400)* compared with wild type. *dpy-19(mu78)* animals are not significantly Dumpy at the time of the Q migrations.

located in bilaterally symmetrical positions on either side of the animal. This places the Q cells in similar positions within a row of epidermal cells, V1-V6, with QL and QR just anterior of V5L and V5R, respectively (Fig. 1A,G,H). From 1 to 3 hours after hatching, QL and QR migrate: QL towards the posterior and QR towards the anterior (Fig. 1A). When viewed with Nomarksi optics, only cell nuclei are visible in *C. elegans*. In order to see the entire Q cell, we examined the cells in *clr-1(e1745ts)* mutants, in which many cell outlines are visible (Hedgecock et al., 1990). We observed that the first step of the Q cell migrations is the growth of a distinct cytoplasmic protrusion in the direction that the whole cell will migrate (Fig. 1C,D; J. Austin and C. K., unpublished). We also used two other, independent methods to reveal the shape of the Q cells: a MIG-2::GFP membrane-localized reporter construct that is expressed in the Q and V cells (Zipkin et al., 1997) and a cytoplasmic UNC-73::GFP reporter (Steven et al., 1998). Using MIG-2::GFP, we were able to observe the shape of the Q cells over time. At hatching, QL and QR appear identical to one another and similar in shape to the V cells (Fig. 1G,H). By one hour after hatching, QL has sent a protrusion dorsally and toward the posterior whereas QR has sent a protrusion dorsally and toward the anterior (Fig. 1I,J). We will refer to this first asymmetrical difference as the posterior and anterior polarization of the Q cells. At 2 hours, the Q cells have clearly begun to migrate, moving slightly dorsally past the neighboring V cells. The Q cells continue to migrate, sometimes with a trailing ventral process (e.g. Fig. 1L). At 3.5 hours after hatching, when QR is dorsal to V4 and QL is dorsal to V5, the Q cells divide (Fig. 1M,N). (Some researchers have used the term 'Q migration' to refer to the migrations of the Q cells and their descendants. In this paper, 'Q migration' refers strictly to the migrations of QL and QR. The subsequent *mab-5*-dependent migrations that occur after QL and QR divide are referred to as the 'Q descendant migrations.')

Mutations in *unc-40*, *dpy-19* and *unc-73* block the nuclear migration of QL and QR

To learn more about the mechanisms that generate the asymmetry of the Q cell migrations, we examined our existing collection of cell migration mutants to find genes that are required for the correct migration of QL and QR. We found that mutations in *unc-40*, *dpy-19* and *unc-73* prevent the Q cells from migrating. We quantified the extent of these migrations by measuring the separation of the Q cell nuclei along the A/P axis at 2.5-3.5 hours. At this time in wild-type animals, the Q cells have moved approximately 25 μm apart from one another. By contrast, in *unc-40*, *dpy-19* and *unc-73* mutants, QL and QR are still in similar A/P positions (Fig. 2).

Mutations in *unc-40* randomize the direction of Q cell polarization

To learn how these mutations affected the leading protrusions of the Q cells, we used MIG-2::GFP to outline the Q cell membrane. In wild type animals at 2-3 hours after hatching, QL and QR had clearly migrated in opposite directions (Fig. 1K,L). In *unc-40* mutants at this time, both QL and QR had progressed from their starting shapes (similar to Fig. 1G,H), but showed a wide range of irregular cell outlines. Usually the Q cells remained rounded at their ventral edge and sent variably shaped protrusions dorsalwards. We saw QL cells that were polarized weakly towards the posterior (Fig. 3A), not obviously polarized (Fig. 3B) or polarized weakly towards the anterior (Fig. 3C). QR had similar polarization defects (e.g. Fig. 3D). We gauged the degree of polarization by noting the position of the dorsal-most protrusion relative to other cells. Overall, in *unc-40(e1430)*

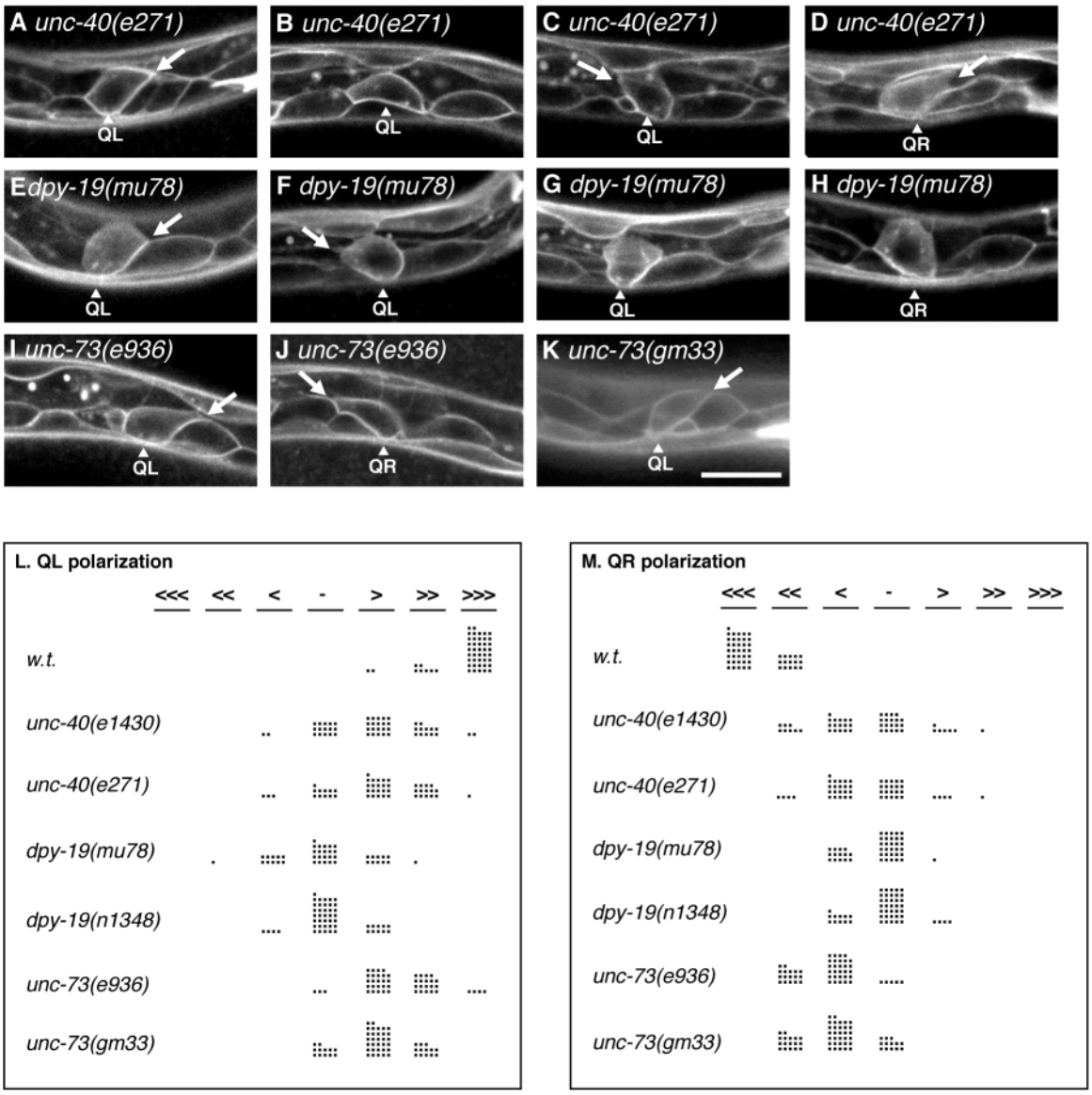

Fig. 3. Polarization of QL and QR in *unc-40*, *dpy-19* and *unc-73* mutants. (A-K) Examples of Q cell shape in *unc-40*;*mig-2::GFP*, *dpy-19*;*mig-2::GFP* and *unc-73*;*mig-2::GFP* animals at 2 hours after hatching (compare with wild type, Fig. 1K,L). Arrows indicate the dorsal leading edge, where apparent. For I-K, similar cell shapes are seen in *unc-73; unc-73::GFP*. (L,M) Summary of the distance the Q cells extend towards the anterior and posterior 2-3 hours after hatching. Each dot represents a single animal. The distance reached by the Q cells was scored relative to neighboring V cells as described in Materials and Methods. Data in L and M were collected by visualizing the shape of Q using MIG-2::GFP for *dpy-19* and *unc-40* mutants and UNC-73::GFP for *unc-73* mutants. *n*=50 animals for each strain. Scale bar: 10 μm.

mutants, 29% of QL cells showed no clear direction of polarization and 4% were misdirected towards the anterior (Fig. 3L). Similarly, 38% of QR cells were unpolarized and 14% of QR cells were incorrectly polarized towards the posterior (Fig. 3M). Thus, in *unc-40* mutants, either Q cell could point in either direction. There was no correlation between the shape of the QL and QR cells in an individual animal (data not shown).

The UNC-40/DCC receptor is required for many cell and axon migrations in *C. elegans*. It has been shown that *unc-40* can act cell autonomously to orient axon outgrowth and that UNC-40::GFP is expressed in many of the cells that require *unc-40* for D/V guidance, including the Q cells (Chan et al., 1996). We confirmed that UNC-40::GFP is expressed strongly in the Q cells during their migration (data not shown), suggesting that UNC-40 may act as the receptor or part of the receptor that orients the QL and QR migrations in opposite directions along the A/P axis.

Single Q cells can polarize in different directions over time in *unc-40* mutants

The wide range of Q cell shapes that we saw in *unc-40(–)* animals could have reflected two different kinds of underlying phenotype. One possibility was that in any individual, the Q cell polarized in one direction, with the variability arising across different individuals. The other possibility was that each Q cell in each animal was able to polarize in multiple directions over time. To distinguish these possibilities, we observed individual Q cells from 0 to 3 hours after hatching. In many

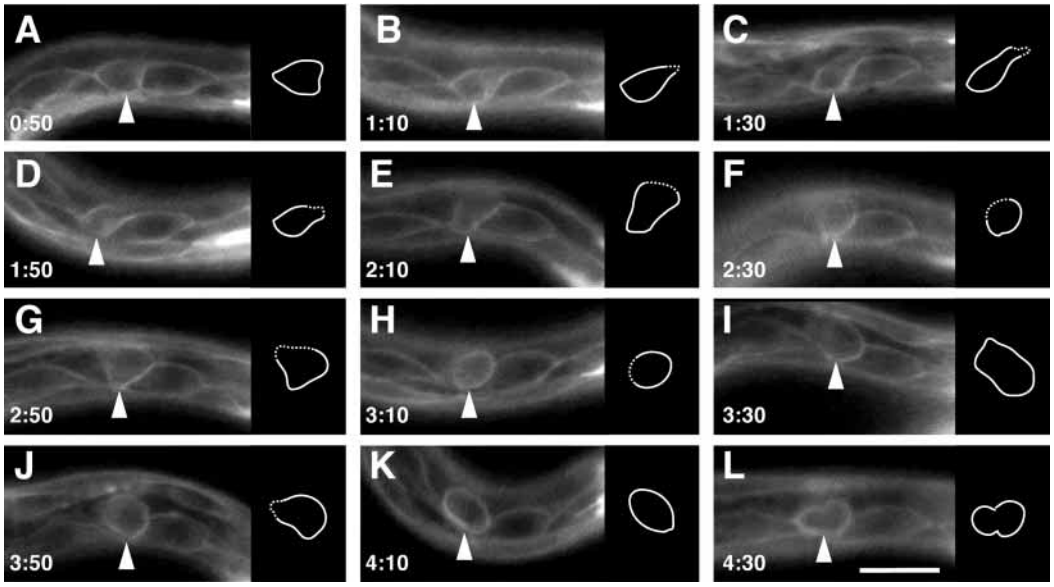

Fig. 4. A single Q cell can polarize in multiple directions over time in an *unc-40* mutant. (A-L) Fluorescent images showing Q cell shape were collected every 20 minutes in an *unc-40(e1430);mig-2::GFP* animal. Tracings of the Q cell are shown to the right of each image. When the edge of the Q cell was out of focus or blurred by motion of the worm, broken lines indicate estimates of the cell shape. Fluorescent time-lapse imaging sometimes slowed the rate of development (the Q cell shown here divided about 1 hour later than normal), but polarization reversals occurred in animals with normal developmental rates as well (16/31 *dpy-19* or *unc-40* mutant animals had normal timing of the Q division, and we saw polarization reversals in 3 out of these 16 animals). In addition, fluorescent imaging caused delayed development in 2/4 wild-type animals, yet we never saw polarization reversals in wild type.

animals, a single Q cell alternately exhibited an irregular, unpolarized shape and polarization in a single direction. However we also found that a single Q cell could point in multiple directions (compare Fig. 4C with 4I). Overall, in 3/11 *unc-40(e1430)* mutants, we observed QL cells that polarized first in one direction and then another.

The Q cell migrations do not require UNC-6, the known UNC-40 ligand

UNC-6/netrin is expressed along the ventral midline and is thought to function as a ligand for UNC-40 in guiding D/V migrations (Wadsworth et al., 1996). We tested whether UNC-6 was also required for the A/P migrations of the Q neuroblasts. We found that in the null allele *unc-6 (ev400)* (Ishii et al., 1992), the Q cells still migrated almost as far as they do in wild type (Fig. 2). Using MIG-2::GFP, we confirmed that Q cell polarization in *unc-6* mutants was also normal (data not shown). We also tested whether UNC-5, the putative co-receptor in D/V guidance, was required for the Q cell migrations. We found that *unc-5* mutants also had almost normal Q cell migrations (Fig. 2); thus UNC-5 does not appear to be a part of the UNC-40-dependent Q guidance system. Finally, given the proposed role of UNC-40 in netrin avoidance (Chan et al., 1996; Hong et al., 1999), the Q cell migration defect seen in an *unc-40* mutant might be the result of these cells inappropriately responding to an UNC-6 signal that they would normally ignore. To test this, we asked whether a mutation in *unc-6* could suppress the phenotype caused by a mutation in *unc-40*. We found that it could not (Fig. 2), implying that the role of UNC-40 in the Q migrations is completely independent of UNC-6. Thus, of the known genes involved in the *C. elegans* netrin guidance system, only *unc-40* is also required for L/R asymmetry of the Q cells.

Mutations in *dpy-19* also randomize the direction of Q cell polarization

As observed in *unc-40* mutants, the Q cells in *dpy-19* mutants did not extend projections as far as in wild type and these projections were sometimes misdirected (Fig. 3). QL polarized weakly towards the posterior (Fig. 3E), weakly towards the anterior (Fig. 3F) or was irregularly shaped (Fig. 3G). QR was similarly affected (Fig. 3H). In the null *dpy-19* allele, *n1347n1348* (see below), QL showed no clear direction of polarization in 72% of animals and projected anteriorly in 8% of animals. Similarly, QR lacked clear polarization in 70% of animals and projected incorrectly towards the posterior in 8% of animals. Like mutations in *unc-40*, mutations in *dpy-19* can cause the Q cells in a single animal to point in different directions over time. In time-lapse video experiments similar to those described for *unc-40*, we saw polarization towards both the anterior and posterior at different times in QL in 4/11 animals and in QR in 3/11 animals. Overall, the Q cell phenotype of *dpy-19* mutants was quite similar to that of *unc-40* mutants, suggesting that these genes might function in a common pathway.

DPY-19 is a novel transmembrane protein

dpy-19 was cloned using a transposon-insertion allele to identify a predicted gene (F22B7.10) that had previously been sequenced by the *C. elegans* sequencing project (S. Collums and R. Plasterk, personal communication). By isolating cDNAs corresponding to F22B7.10 we were able to correct a mis-predicted splice junction for the first exon for this gene (see Materials and Methods). We confirmed that F22B7.10 was *dpy-19* by identifying mutations in all known *dpy-19* alleles (Fig. 5A). *n1347n1348*, the allele with the most severe phenotype, contained an approximately 9 kb deletion that removed most of the *dpy-19* coding region. The *dpy-19* transcript was not detected in *n1347n1348* by northern analysis (Fig. 5B), confirming that this allele represents the null phenotype of *dpy-19*.

The sequence of *dpy-19* defines a novel protein with 13 hydrophobic domains, suggesting that it is a transmembrane protein that crosses the membrane multiple times. *dpy-19*

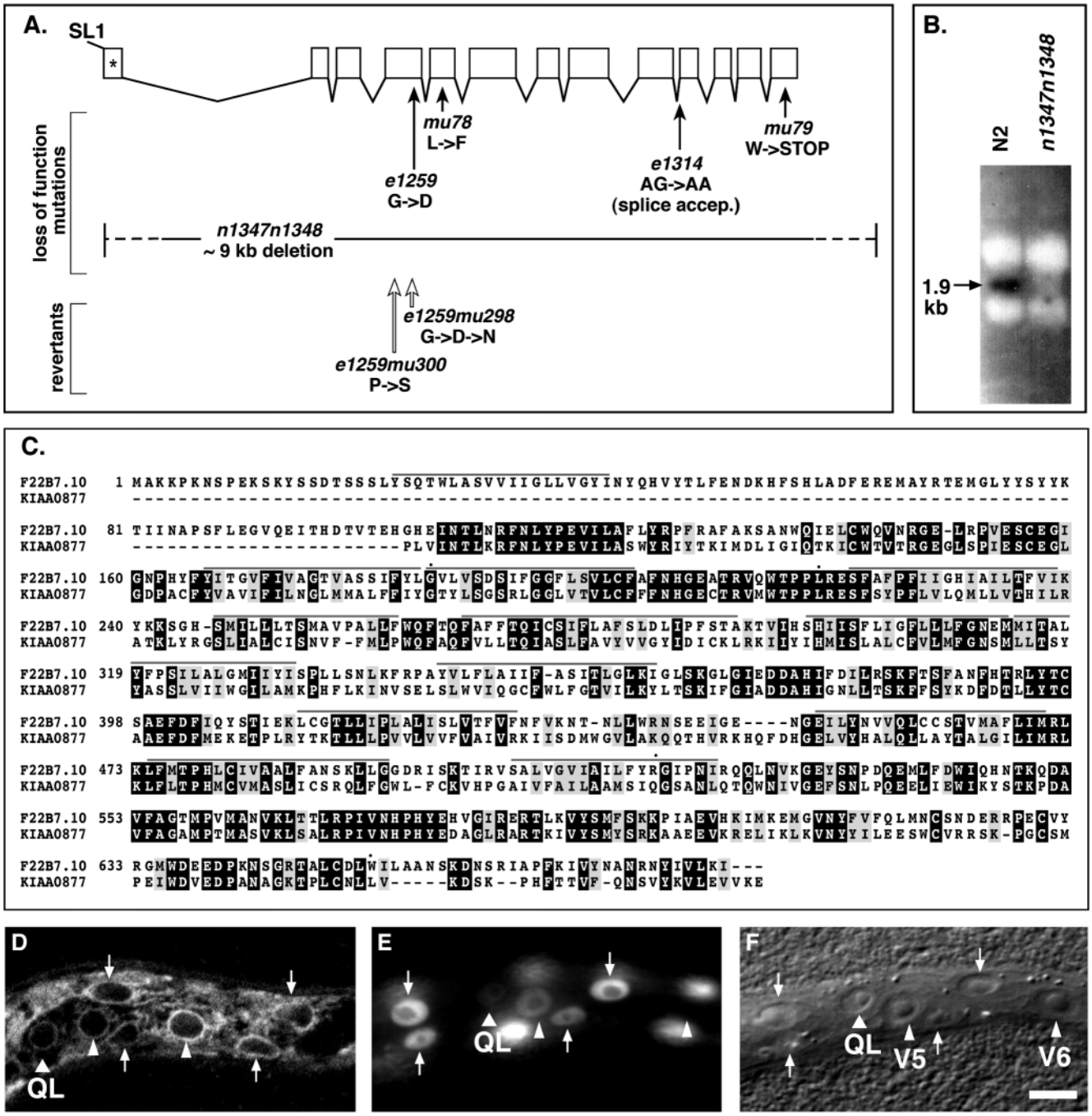

Fig. 5. Cloning of *dpy-19*. (A) Schematic diagram showing intron and exon boundaries in *dpy-19*. Black arrows mark sites of point mutations found in four different *dpy-19* alleles. Open arrows mark sites of mutations found in intragenic revertants of *dpy-19(e1259)*. Exact mutation sites: *mu78*(L218->F), *e1259*(G185->D), *e1314*(splice acceptor mutation disrupts protein after R517), *mu79*(W653->STOP), *e1259mu298*(G185->N), *e1259mu300*(P127->S, G185->D). *, revised first exon that was not predicted by Genefinder analysis of genomic sequence (*C. elegans* Sequencing Consortium). (B) Northern blot of total RNA probed with sequences from the *dpy-19* gene. N2 lane contains wild-type RNA and *n1347n1348* lane contains RNA from the deletion allele, *dpy-19(n1347n1348)*. (White bands reflect a decrease in background from excess rRNA.) (C) Alignment of DPY-19/F22B7.10 and the human full-length cDNA KIAA0877 (Genbank Accession: AB020684, Unigene cluster Hs. 11217.). DPY-19 and KIAA0887 are 41% identical and 61% similar over 547 amino acids. Gray lines above F22B7.10 sequence indicate position of 13 potential membrane spanning domains predicted by TMPred (Hofmann and Stoffel, 1993). •, the position of the loss of function mutations described in (A). (D) Expression of GFP-tagged DPY-19 in QL and surrounding cells. Rings of GFP expression are coincident with cell nuclei outlines. This construct fully rescues mutations in *dpy-19* (see Materials and Methods). (E,F) Expression of nuclear-localized GFP under control of the *dpy-19* promoter. (E) shows GFP expression faintly in QL and strongly in surrounding epidermal cells. (F) shows a Nomarski image of the same worm. In animals containing the array, 5/15 QL cells and 9/18 QR cells expressed GFP faintly during the time of the Q migrations. In D-F, arrows mark dorsal (hyp7) and ventral (P) epidermal nuclei and arrowheads mark lateral (V) epidermal nuclei. The lack of expression in V6 in E is presumed to be the result of sporadic loss of the extrachromosomal array carrying the GFP reporter since other animals showed strong expression in V6. Scale bar: 5 μm.

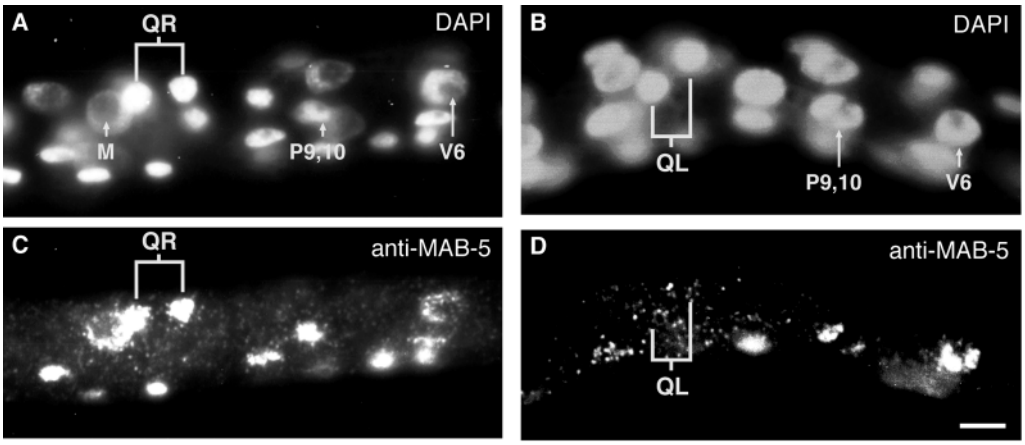

Fig. 6. MAB-5 protein expression in the Q descendants. (A,C) QR.a and QR.p inappropriately expressing MAB-5 in a *dpy-19(mu78)* mutant. (B,D) QL.a and QL.p failing to express MAB-5 in a *dpy-19(mu78)* mutant. DAPI (A,B) stains all nuclei. M, P9/10, and V6 are shown for reference. Out of focus MAB-5 staining is in posterior body muscle and ventral cord motoneurons, cells that normally express MAB-5. (E) Percentage of worms with anti-MAB-5 staining in the Q.a and Q.p descendants. Animals were fixed and stained 3.5-5.5 hours after hatching. To control for worm permeabilization and quality of antibody staining, we scored only animals in which V6 showed anti-MAB-5 staining. Strong, Q descendants staining as bright or brighter than V6 in the same animal; Weak, Q descendants staining, but not as bright as V6. % desc. post., percentage of animals with QL.pax descendants posterior to V4.a; n.d., not determined. Alleles used for double mutants with *egl-20*: *egl-20(n585)*, *unc-40(e271)*, *dpy-19(mu78)* and *unc-73(e936)*. Scale bar: 5 μm.

E

	QL					QR				
	MAB-5 staining				% desc.	MAB-5 staining				% desc.
genotype	% none	% weak	% strong	n	post.	% none	% weak	% strong	n	post
w.t.	0.0	0.0	100.0	94	100.0	100.0	0.0	0.0	170	0.0
unc-40(e271)	20.7	41.4	37.9	29	43.8	89.3	10.7	0.0	28	0.0
dpy-19(mu78)	40.0	25.7	34.3	35	38.4	84.8	3.0	12.1	33	6.0
unc-73(e936)	6.7	6.7	86.7	90	95.8	98.8	1.3	0.0	80	0.0
unc-73(gm33)	22.9	10.4	66.7	48	n.d.	97.1	0.0	2.9	35	n.d.
egl-20	100.0	0.0	0.0	27	0.0	100.0	0.0	0.0	27	0.0
unc-40; egl-20	100.0	0.0	0.0	50	n.d.	100.0	0.0	0.0	42	n.d.
dpy-19; egl-20	100.0	0.0	0.0	50	n.d.	100.0	0.0	0.0	54	n.d.
unc-73; egl-20	100.0	0.0	0.0	50	n.d.	100.0	0.0	0.0	31	n.d.

shows significant homology to a human cDNA (Fig. 5C), but does not contain any known sequence motifs.

In an attempt to identify proteins that might interact with DPY-19, we screened approximately 500,000 genomes for suppressors of *dpy-19(e1259)* (see Materials and Methods). All eight independent suppressor mutations were tightly linked to *dpy-19* and behaved genetically as if they were intragenic. We sequenced the *dpy-19* region in the two strongest suppressors and found that both were in fact intragenic. The strongest suppressor, *e1259mu298*, contained a second mutation in the same codon that was originally mutated in *e1259*. The other suppressor, *e1259mu300*, contained a second mutation located upstream of the *e1259* mutation (Fig. 5A). Because all eight suppressors are likely to be intragenic and because our mutagenesis was extensive enough to find a second mutation in the originally mutated codon, we suspect that there are few or no extragenic targets in which a point mutation can compensate for a reduction in *dpy-19* activity.

DPY-19::GFP is expressed in Q

In order to learn which cells express *dpy-19*, we inserted GFP at the predicted 5′ and 3′ ends of the gene. These GFP-tagged constructs showed full rescuing activity and displayed similar expression patterns (see Materials and Methods). At the time of the Q cell migrations, many cells faintly expressed GFP-tagged DPY-19 in a reticular pattern, with the brightest staining localized at the periphery of cell nuclei (Fig. 5D). To more clearly identify the cells expressing *dpy-19*, we made a transcriptional fusion that used the same upstream region as the rescuing GFP-tagged constructs, but with the *dpy-19* coding sequence replaced by a nuclear-localized GFP-coding sequence. This construct was expressed faintly in QL and QR, more strongly in the neighboring epidermal cells (dorsal hyp7 cells, ventral P cells and lateral V cells), and in dorsal and ventral body muscle cells (Fig. 5E,F).

dpy-19 is not required for other cell migrations

To see if *dpy-19* is generally required for cell motility, we examined *dpy-19* mutants for defects in other cell and axon migrations. No defects in the embryonic migrations of HSN, CAN, M and ALM were seen in *dpy-19(n1347n1348)* animals (n=35) and no defects in the postembryonic migrations of the distal tip cells (DTCs) or male linker cell were seen in *dpy-19(mu78)* animals (n=50). Thus, although *dpy-19* and *unc-40* mutants have similar defects in the Q cells, *unc-40* mutants have many other defects (Hedgecock et al., 1990) that are not present in *dpy-19* mutants.

Mutations in *unc-73*/trio prevent the Q cells from fully polarizing

Mutations in *unc-73* also blocked the Q migrations and disrupted the polarized leading processes (Fig. 3I-M). In animals carrying the weak *unc-73* allele *e936*, 6% of the QL cells were unpolarized and 9% of the QR cells were unpolarized. In animals containing the stronger *unc-73* allele, *gm33*, 24% of QL cells and 26% of QR cells were unpolarized.

Although many cells in *dpy-19*, *unc-40* and *unc-73* mutants were scored as having no clear polarity, the unpolarized phenotype (scored as '–' in Fig. 3L,M) seen in *unc-73(gm33)* mutants was qualitatively different from that seen in *dpy-19* and *unc-40* mutants: in *unc-73* mutants the Q cells were almost always round rather than irregularly shaped. Also, in contrast to *unc-40* and *dpy-19* mutants, we never saw any *unc-73* mutants in which the Q cells were pointed in the wrong direction. Although relatively few cells polarize in the wrong direction in *dpy-19* and *unc-40* mutants, the complete absence of incorrectly polarized cells seen in *unc-73* mutants was significantly different from the phenotypes of *dpy-19* and *unc-40* mutants ($P \leq 0.007$, Fisher exact test).

The phenotype of *unc-73* mutants also demonstrates that the polarization and migration of the Q cells are separable events. At hatching, the QL cell is pointed slightly anteriorly (Fig. 1G,H), with its shape mirroring the shape of its sister cell V5. In *unc-73* mutant animals, QL still points anteriorly at hatching, but over the next 3 hours, it can reorient and point towards the posterior without showing any signs of migration (for example, Fig. 3I). This phenotype illustrates that polarization in the Q cells can occur without migration.

Finally, consistent with the hypothesis that *unc-73* acts within the Q cells to allow their outgrowth and migration, an UNC-73::GFP fusion was expressed strongly in Q at the time of its migration (Fig. 1E,F; Steven et al., 1998).

unc-40, *dpy-19* and *unc-73* mutants cause defects in MAB-5 expression in the Q descendants

We next asked what effect these mutations would have on the second aspect of the Q cells' L/R asymmetry, MAB-5 expression. We stained animals with anti-MAB-5 antibodies when the Q cells had divided once. MAB-5 is normally expressed in the daughters of QL, but not in the daughters of QR. We found that mutations in all three genes described above also partially randomized MAB-5 expression (Fig. 6). In *unc-40* and *dpy-19* mutants, the QL descendants often failed to express MAB-5. At a lower frequency, the QR descendants sometimes expressed MAB-5, a phenotype never observed in wild type. In the weak *unc-73* allele, *e936*, only a small percentage of animals failed to express MAB-5 in QL, but in the stronger *unc-73* allele, *gm33*, this defect was more pronounced (Fig. 6E).

Because *mab-5* is necessary and sufficient for posterior migration in the Q descendants, the defects in MAB-5 expression described above were expected to result in defects in the migration in the Q descendants. As predicted, we found that in *unc-40* and *dpy-19* mutants, the QL descendants sometimes migrated anteriorly and the QR descendants sometimes remained in the posterior (Fig. 7 and Hedgecock et al., 1990). At a lower frequency, the QL and QR descendants were misplaced in *unc-73* mutants (Fig. 7 and Way et al., 1992). In all mutants, the frequency of animals in which the QL or QR descendants expressed MAB-5 was well correlated with the corresponding frequency of animals in which the Q descendants remained in the posterior (Fig. 6E).

We confirmed genetically that the mis-positioned Q descendants in *unc-40*, *dpy-19* and *unc-73* mutants were caused by the incorrect expression of MAB-5. In the *unc-40; mab-5*, *mab-5 dpy-19* and *unc-73; mab-5* double mutants, the QL and QR descendants always migrated anteriorly (Fig. 7).

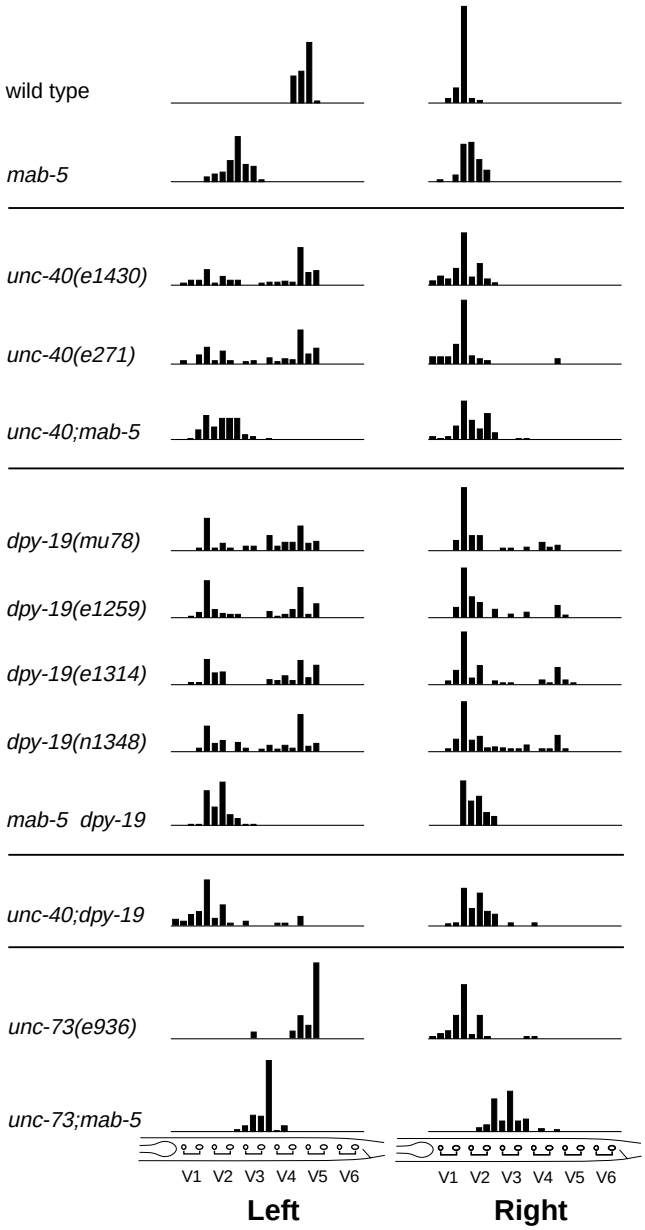

Fig. 7. Final position of the Q descendants. Histograms show the distribution of the final positions of the QL.pax and QR.pax cells (see * in Fig. 1B) relative to the daughters of the epidermal cells V1-V6 (shown at the bottom). All graphs have the same vertical axis scale as wild type. Allele names for double mutants: *unc-40(e271);mab-5(e2088)*, *mab-5(e2088);dpy-19(mu78)*, *unc-40(e271);dpy-19(mu78)*, *unc-73(e936);mab-5(e2088)*. *n*=50 worms for each genotype, except *mab-5 dpy-19* right side, *n*=100.

Although *dpy-19* and *unc-40* are required for QL and QR to migrate, these genes are not required for the Q descendants to migrate. In the absence of MAB-5 (in the *unc-40; mab-5* and *mab-5 dpy-19* double mutants), the QL and QR descendants migrate as far toward the anterior as they did in *mab-5* single mutants (Fig. 7). By contrast, in the *unc-73; mab-5* double mutant, the QR descendants ended their migrations at intermediate positions on the A/P axis (Fig. 7). Therefore, *unc-73* must have two functions in the Q lineage: it is required for the

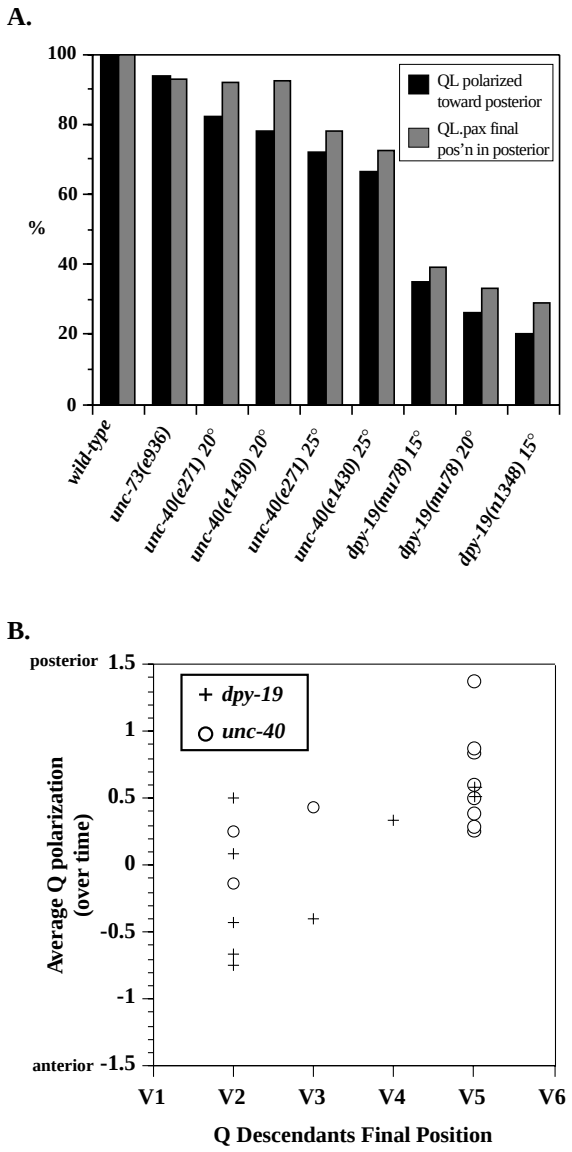

Fig. 8. Direction of Q cell polarization correlates with final position of Q descendants. (A) Animals from the same staged population were scored at 2 hours after hatching to determine the percentage of QL cells that pointed towards the posterior and at 11 hours after hatching to determine the percentage of QL.pax descendants that remained in the posterior (indicating that the QL descendants expressed MAB-5). To allow visualization of the shape of the QL cells, all strains in this graph also contained *mig-2::GFP*, except *unc-73(e936)*, which contained *unc-73::GFP*. QL.pax descendants were scored as 'posterior' if they were posterior to V4.a. *n*=50 worms for each genotype. (B) Polarization over time towards the posterior correlates with the Q descendants remaining in the posterior. *dpy-19(mu78)*;*mig-2::GFP* and *unc-40(e1430)*; *mig-2::GFP* animals were examined every 20 minutes, as in Fig. 4. The cell shape of QL and QR at each time point was assigned an integer score from –2 to +2, corresponding to the degree of polarization toward the anterior (–) or posterior (+). The average of these polarization scores for each animal is plotted versus the final position of the Q descendants in that animal. The unpredictability of the final positions for Q cells with intermediate levels of polarization over time may reflect the relatively coarse resolution of our assay for polarization.

migrations of QL and QR and also for the full extent of the Q descendant migrations toward the anterior when *mab-5* is OFF.

In both *unc-40* and *dpy-19* single mutants, *mab-5* was more likely to be OFF than ON in both QL and QR. We also examined MAB-5 expression in *unc-40; dpy-19* double mutants, and found that it was almost always OFF in both cells (Fig. 7). This suggests that the inappropriate expression of MAB-5 in QR might be triggered when the activity of this polarizing system is low, but not completely eliminated. We were unable to examine cell shape in these animals because their viability was too poor.

MAB-5 expression in the Q cell migration mutants still requires EGL-20/Wnt

In wild-type animals, expression of MAB-5 in QL requires a Wnt signaling pathway. We tested whether MAB-5 expression in Q in *unc-40*, *dpy-19* and *unc-73* mutants was still dependent on *egl-20*, the gene that encodes the Wnt signal. We stained *unc-40; egl-20*, *dpy-19; egl-20* and *unc-73; egl-20* mutants with MAB-5 antibodies and found that MAB-5 protein was absent in the Q descendants (Fig. 6E). Thus *unc-40*, *dpy-19* and *unc-73* mutants still require *egl-20*/Wnt to express MAB-5, implying that these mutations cause incorrect expression of MAB-5 by altering the normal Wnt signaling process.

The shape of the Q cell is correlated with the final position of the Q descendants

Because *unc-40*, *dpy-19* and *unc-73* mutations all caused randomization of both polarization and MAB-5 expression in the Q cells, we wondered if these two phenotypes were correlated. To investigate this, we tested multiple alleles of all three mutants at multiple temperatures and found that, on both the left and the right, the frequency with which the Q cell polarized toward the posterior was strongly correlated with the frequency with which the Q descendants expressed MAB-5 and migrated posteriorly (Fig. 8A and data not shown). We tested whether the trend seen in populations of animals would hold true for individual *dpy-19*(–) or *unc-40*(–) animals, i.e. when a Q cell points the wrong way does it then mis-express MAB-5? Because the Q cell shape in *dpy-19* and *unc-40* mutants varied over time (Fig. 4), we considered several models for how the profile of the Q polarization might predict MAB-5 expression in the Q descendants. Our first model was that Q cells that pointed toward the posterior at any time would subsequently turn on *mab-5*. We tested this by picking individual *dpy-19*(–) animals at 2.5 hrs after hatching in which QL or QR were polarized toward the posterior. In these selected animals, the Q descendants still frequently migrated anteriorly (8/21 for QL and 6/7 for QR), thereby ruling out this model. Our second model was that the shape of the Q cell at some particular time, e.g. right before the division of Q, would correlate with the expression of MAB-5. However, no such critical time point was apparent from the experiments in which we followed the shape of the Q cells over time (data not shown). Our third model was that those Q cells that spent the most time polarized towards the posterior would also be the most likely to express MAB-5. We found that this was the case; animals with the strongest tendency over time to point towards the posterior were the ones in which the Q descendants remained in the posterior (Fig. 8B).

DISCUSSION

By studying the migration of the Q neuroblasts in *C. elegans* we can address three basic developmental questions: (1) how L/R asymmetries are specified; (2) how cells orient themselves along the A/P axis in response to extracellular cues; and (3) how *Hox* gene expression is regulated in migrating cells. In this paper we show that a system involving *unc-40*, *dpy-19* and *unc-73* coordinates these processes.

UNC-40 and DPY-19 are required to orient the Q cells and to express MAB-5 correctly in the Q cell descendants

In both *unc-40* and *dpy-19* mutants the earliest detectable defect in the Q cells is their failure to orient and polarize correctly. Instead, QL and QR seem to cast about, forming short-lived, small processes that point in multiple directions and the Q cells fail to migrate appreciably in these mutants. In addition, QL sometimes fails to express MAB-5 and QR sometimes inappropriately expresses MAB-5. As a consequence, the Q descendants sometimes migrate incorrectly.

In D/V guidance, *unc-40* acts cell autonomously to orient the migration of many cells and axons. Moreover, UNC-40::GFP is expressed brightly in the Q cells at the time of their migration. Thus, *unc-40* is also likely to function as a receptor in orienting the A/P migration of QL and QR. The ligand for UNC-40 in D/V guidance is UNC-6/netrin, but since *unc-6* is not required for the Q cell migration, we propose that a currently unidentified protein functions as a ligand for UNC-40 in the Q cells. The vertebrate *unc-40* homolog, DCC, is also expressed in some neurons that do not appear to respond to netrin (Fazeli et al., 1997; Keino et al., 1996), suggesting there may be another ligand in vertebrates.

Two simple models can explain how *unc-40* might function in polarizing QL and QR. The first model postulates that the two Q cells are identical, in that they both seek out the same target, but that the location of the target is different on the two sides of the animal (Fig. 9A). In the second model, the difference between the Q migrations on the left and right sides is caused by the Q cells themselves, not their surroundings. For example, QL might be attracted toward a localized signal along the A/P axis, while QR is repelled (Fig. 9B). In this model, the role of UNC-40 in the Q cells would be analogous to its role in D/V migration, in which it is required for growth towards and away from UNC-6/netrin signals (Chan et al., 1996; Kim et al., 1999). In D/V migration, UNC-40/DCC may form co-receptors with UNC-5, which causes netrins to repel rather than attract growing axons (Hong et al., 1999). Likewise, different UNC-40 co-receptor complexes might be expressed differently in the two Q cells to enable them to respond differently to the same extracellular cues.

dpy-19 encodes a novel protein, but the similarity of the Q phenotypes in *dpy-19* and *unc-40* mutants suggests that *dpy-19* may function in the same cell signaling pathway as *unc-40*. DPY-19 could function either in the production of or the response to a signal that polarizes the Q cells. DPY-19 appears to function fairly specifically in Q cell migrations; however, it could also function redundantly in other cell processes. The similarity of *dpy-19* to a human cDNA suggests that DPY-19 may have an evolutionarily conserved role in cell signaling.

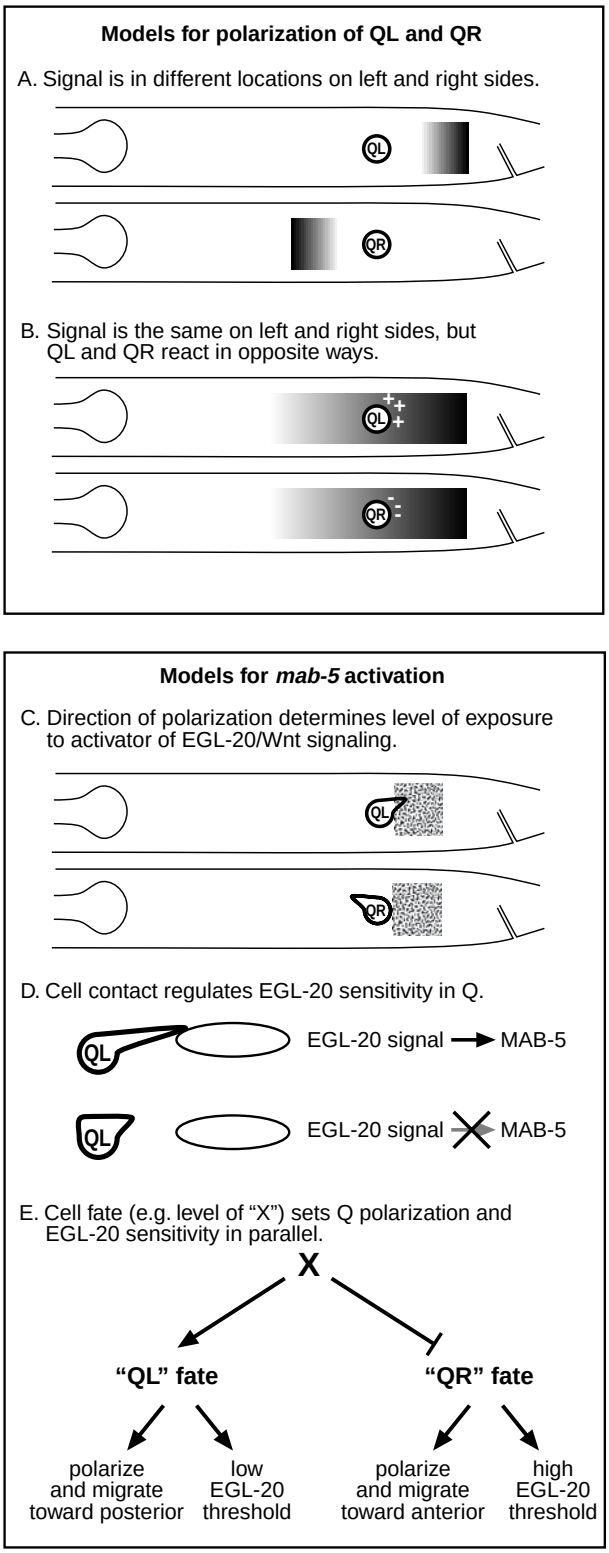

Fig. 9. Models for the polarization of the Q cells and the control of MAB-5 expression.

unc-73 is required for the migration of QL and QR

We found that mutations in *unc-73* partially block polarization of the Q cells and prevent their migration, but do not randomize

the direction of polarization. Thus, *unc-73* may function in organizing the cytoskeleton in migrating cells in response to extracellular cues. Mutations in *unc-73* cause many cell and axon migration defects (Desai et al., 1988; Forrester and Garriga, 1997; Hedgecock et al., 1990; McIntire et al., 1992). UNC-73 is a member of the Trio family of proteins (Steven et al., 1998), which has been implicated in cytoskeletal signaling and axon guidance in vertebrates and *Drosophila* (Awasaki et al., 2000; Bateman et al., 2000; Debant et al., 1996; Liebl et al., 2000; Newsome et al., 2000). Trio interacts physically and genetically with axon guidance receptor phosphatases and kinases, and the GEF domains within Trio can in turn regulate the actin cytoskeleton via their effects on Rho-family GTPases (reviewed in Hall, 1998). Our findings indicate that UNC-73/Trio functions in polarization of the Q neuroblasts. Although we cannot rule out the possibility that a complete elimination of *unc-73* function would cause the Q cells to polarize randomly, it seems most likely that the role of *unc-73* in the Q cell polarization is distinct from that of *dpy-19* and *unc-40*. *dpy-19* and *unc-40* are required for the Q cells to choose a direction in which to polarize, while *unc-73* appears to be required only for the Q cells to carry out their polarization and migration.

Although it is unknown what receptors might interact with UNC-73 in the Q cells, there is a good candidate GTPase that could function downstream of the GEF domains in UNC-73. MIG-2, which defines a subclass of the Rho-family, is required for the migration of the Q cells. Mutations in *mig-2* result in shortened migrations of QL and QR, similar to the phenotype of *unc-73* mutants. Because both the activating and null alleles of *mig-2* cause similar phenotypes in the Q cells, GDP-GTP cycling of MIG-2 may be required for the Q cells to migrate (Zipkin et al., 1997). In addition, the first GEF domain of *Drosophila* Trio promotes GDP release from the recently identified Mtl, the *Drosophila* homolog of *mig-2* (Newsome et al., 2000). Thus, MIG-2 may be a downstream target of UNC-73 in the Q cells. The partial suppression of *unc-73(e936)* by *muIs28*, the multicopy array of GFP-tagged *mig-2*(+) (see Materials and Methods), is consistent with this hypothesis.

Identifying the steps in cell polarization

By observing single animals over time, we found that mutations in *dpy-19* and *unc-40* cause the Q cells to polarize in multiple directions. This suggests the possibility that in these mutants the Q cells are still activated to polarize and migrate, but lack the cues setting their direction. Such a phenotype may be analogous to the cell polarization phenotypes seen during *Saaccharomyces cerevisiae* budding and shmoo formation. Mutations in bud site selection genes, such as the GTPase Bud1, cause yeast cells to form normal budding polarizations, but pointed in the wrong direction (Chant and Herskowitz, 1991). The shape of the Q cells seen in *unc-40* and *dpy-19* mutants is similar to the multiple protrusions in different directions formed by *S. cerevisiae* cells in a uniform concentration of pheromone (Segall, 1993). Since Rho-family GTPases are involved in both yeast cell polarization (Johnson and Pringle, 1990) and Q cell polarization (Zipkin et al., 1997), a common molecular mechanism may link the proteins that mark the direction of polarization to the cytoskeletal changes that allow polarization.

Models for activation of MAB-5

Previous studies suggest that QL but not QR activates MAB-5 expression during normal development because QL and QR have different response thresholds to EGL-20, which is produced in the posterior body region near the tail (Whangbo and Kenyon, 1999). Mutations in *unc-40* and *dpy-19* randomize the L/R asymmetrical pattern of MAB-5 expression. We found that the probability that a Q cell would express MAB-5 correlated with the relative amount of time it spent pointing toward the posterior. Why should such a correlation exist? One possibility is that polarization towards the posterior increases the exposure of the cells to an activator of Wnt signaling that is located posterior to QL, or decreases its exposure to an anteriorly localized repressor (Fig. 9C). A second possibility is that polarization allows QL or QR to make a stable cell contact that in turn regulates sensitivity to the EGL-20 signal (Fig. 9D). Such a model is attractive because cell contact is known to regulate an EGL-20/Wnt signaling pathway that can activate MAB-5 expression in the cells V5 and V6 (Hunter et al., 1999). Finally, *unc-40* and *dpy-19* could act at the head of a regulatory cascade that governs both Q cell polarization and EGL-20 sensitivity in parallel (Fig. 9E).

In summary, in this study we have found that the L/R asymmetry of the Q cell migration is conferred by a signaling system involving the UNC-40 protein, which also functions to mediate cell and axon migration along the D/V axis. Our findings suggest that UNC-40 mediates L/R migrations in response to a unknown ligand, and moreover that a mechanism exists to make the Q cell migrations immune to the ventrally located UNC-6/netrin ligand. This L/R system, but not the D/V system, requires the evolutionarily conserved DPY-19 protein. The Q cell migrations are also dependent on the UNC-73/Trio protein, which may function to couple the L/R asymmetry to downstream GTPase-regulated cytoskeletal changes. Thus, this study provides an entry point for investigating not only the basis of an L/R asymmetrical cell migration but also the question of how orthogonal migration systems can share components and yet remain separate from one another.

We thank Judith Austin, Jeanne Harris, Julin Maloof, Naomi Robinson, Ilan Zipkin and other Kenyon laboratory members for sharing data, reagents and ideas. We are grateful to Sean Collums, Ronald Plasterk and Mike Finney for sharing unpublished data. Gian Garriga, Robert Steven and Joseph Culotti kindly provided several strains used in this work. Some strains were provided by the *Caenorhabditis* Genetics Center, which is funded by the NIH.

REFERENCES

Awasaki, T., Saito, M., Sone, M., Suzuki, E., Sakai, R., Ito, K. and Hama, C. (2000). The *Drosophila* trio plays an essential role in patterning of axons by regulating their directional extension. *Neuron* **26**, 119-131.

Bateman, J., Shu, H. and Van Vactor, D. (2000). The guanine nucleotide exchange factor trio mediates axonal development in the *Drosophila* embryo. *Neuron* **26**, 93-106.

Brenner, S. (1974). The genetics of *C. elegans*. *Genetics* **77**, 71-94.

Chalfie, M., Thomson, N. J. and Sulston, J. (1983). Induction of neuronal branching in *Caenorhabditis elegans*. *Science* **221**, 61-63.

Chan, S. S., Zheng, H., Su, M. W., Wilk, R., Killeen, M. T., Hedgecock, E. M. and Culotti, J. G. (1996). UNC-40, a *C. elegans* homolog of DCC (Deleted in Colorectal Cancer), is required in motile cells responding to UNC-6 netrin cues. *Cell* **87**, 187-195.

Chant, J. and Herskowitz, I. (1991). Genetic control of bud site selection in

yeast by a set of gene products that constitute a morphogenetic pathway. *Cell* **65**, 1203-1212.

Colamarino, S. A. and Tessier-Lavigne, M. (1995). The axonal chemoattractant netrin-1 is also a chemorepellent for trochlear motor axons. *Cell* **81**, 621-629.

Debant, A., Serra-Pages, C., Seipel, K., O'Brien, S., Tang, M., Park, S. H. and Streuli, M. (1996). The multidomain protein Trio binds the LAR transmembrane tyrosine phosphatase, contains a protein kinase domain, and has separate rac-specific and rho-specific guanine nucleotide exchange factor domains. *Proc. Natl. Acad. Sci. USA* **93**, 5466-5471.

Desai, C., Garriga, G., McIntire, S. L. and Horvitz, H. R. (1988). A genetic pathway for the development of the Caenorhabditis elegans HSN motor neurons. *Nature* **336**, 638-646.

Eisenmann, D. M., Maloof, J. N., Simske, J. S., Kenyon, C. and Kim, S. K. (1998). The beta-catenin homolog BAR-1 and LET-60 Ras coordinately regulate the Hox gene lin-39 during *Caenorhabditis elegans* vulval development. *Development* **125**, 3667-3680.

Fazeli, A., Dickinson, S. L., Hermiston, M. L., Tighe, R. V., Steen, R. G., Small, C. G., Stoeckli, E. T., Keino, M. K., Masu, M., Rayburn, H. et al. (1997). Phenotype of mice lacking functional Deleted in colorectal cancer (Dcc) gene. *Nature* **386**, 796-804.

Forrester, W. C. and Garriga, G. (1997). Genes necessary for *C. elegans* cell and growth cone migrations. *Development* **124**, 1831-1843.

Frohman, M. A. (1993). Rapid amplification of complementary DNA ends for generation of full-length complementary DNAs: thermal RACE. *Methods Enzymol.* **218**, 340-356.

Hall, A. (1998). Rho GTPases and the actin cytoskeleton. *Science* **279**, 509-514.

Harris, J., Honigberg, L., Robinson, N. and Kenyon, C. (1996). Neuronal cell migration in *C. elegans*: regulation of Hox gene expression and cell position. *Development* **122**, 3117-3131.

Hedgecock, E. M., Culotti, J. G. and Hall, D. H. (1990). The unc-5, unc-6, and unc-40 genes guide circumferential migrations of pioneer axons and mesodermal cells on the epidermis in C. elegans. *Neuron* **4**, 61-85.

Hedgecock, E. M., Culotti, J. G., Hall, D. H. and Stern, B. D. (1987). Genetics of cell and axon migrations in *Caenorhabditis elegans*. *Development* **100**, 365-382.

Hofmann, K. and Stoffel, W. (1993). TMbase – a database of membrane spanning proteins segments. *Biol. Chem. Hoppe-Seyler* **347**, 166.

Hong, K., Hinck, L., Nishiyama, M., Poo, M. M., Tessier-Lavigne, M. and Stein, E. (1999). A ligand-gated association between cytoplasmic domains of UNC5 and DCC family receptors converts netrin-induced growth cone attraction to repulsion. *Cell* **97**, 927-941.

Hunter, C. P., Harris, J. M., Maloof, J. N. and Kenyon, C. (1999). Hox gene expression in a single *Caenorhabditis elegans* cell is regulated by a caudal homolog and intercellular signals that inhibit wnt signaling. *Development* **126**, 805-814.

Hutter, H. and Schnabel, R. (1995). Establishment of left-right asymmetry in the *Caenorhabditis elegans* embryo: a multistep process involving a series of inductive events. *Development* **121**, 3417-3424.

Ishii, N., Wadsworth, W. G., Stern, B. D., Culotti, J. G. and Hedgecock, E. M. (1992). UNC-6, a laminin-related protein, guides cell and pioneer axon migrations in C. elegans. *Neuron* **9**, 873-881.

Johnson, D. I. and Pringle, J. R. (1990). Molecular characterization of CDC42, a *Saccharomyces cerevisiae* gene involved in the development of cell polarity. *J. Cell Biol.* **111**, 143-152.

Keino, M. K., Masu, M., Hinck, L., Leonardo, E. D., Chan, S. S., Culotti, J. G. and Tessier, L. M. (1996). Deleted in Colorectal Cancer (DCC) encodes a netrin receptor. *Cell* **87**, 175-185.

Kennedy, T. E., Serafini, T., de la Torre, J. R. and Tessier-Lavigne, M. (1994). Netrins are diffusible chemotropic factors for commissural axons in the embryonic spinal cord. *Cell* **78**, 425-435.

Kenyon, C. (1986). A gene involved in the development of the posterior body region of *C. elegans*. *Cell* **46**, 477-487.

Kim, S., Ren, X. C., Fox, E. and Wadsworth, W. G. (1999). SDQR migrations in *Caenorhabditis elegans* are controlled by multiple guidance cues and changing responses to netrin UNC-6. *Development* **126**, 3881-3890.

Liebl, E. C., Forsthoefel, D. J., Franco, L. S., Sample, S. H., Hess, J. E., Cowger, J. A., Chandler, M. P., Shupert, A. M. and Seeger, M. A. (2000). Dosage-sensitive, reciprocal genetic interactions between the Abl tyrosine kinase and the putative GEF trio reveal trio's role in axon pathfinding. *Neuron* **26**, 107-118.

Maloof, J. N., Whangbo, J., Harris, J. M., Jongeward, G. D. and Kenyon, C. (1999). A Wnt signaling pathway controls hox gene expression and neuroblast migration in *C. elegans*. *Development* **126**, 37-49.

McIntire, S. L., Garriga, G., White, J., Jacobson, D. and Horvitz, H. R. (1992). Genes necessary for directed axonal elongation or fasciculation in C. elegans. *Neuron* **8**, 307-322.

Mello, C. C., Kramer, J. M., Stinchcomb, D. and Ambros, V. (1991). Efficient gene transfer in *C. elegans*: extrachromosomal maintenance and integration of transforming sequences. *EMBO J.* **10**, 3959-3970.

Newsome, T. P., Schmidt, S., Dietzl, G., Keleman, K., Asling, B., Debant, A. and Dickson, B. J. (2000). Trio combines with dock to regulate Pak activity during photoreceptor axon pathfinding in *Drosophila*. *Cell* **101**, 283-294.

Salser, S. and Kenyon, C. (1991). Activation of a *C. elegans Antennapedia* homolog within migrating cells controls their direction of migration. *Nature* **355**, 255-258.

Salser, S. J., Loer, C. M. and Kenyon, C. (1993). Multiple HOM-C gene interactions specify cell fates in the nematode central nervous system. *Genes Dev.* **7**, 1714-1724.

Sambrook, J., Maniatis, T. and Fritsch, E. F. (1989). *Molecular Cloning: A Laboratory Manual*. New York: Cold Spring Harbor Laboratory.

Sawa, H., Lobel, L. and Horvitz, H. R. (1996). The *Caenorhabditis elegans* gene lin-17, which is required for certain asymmetric cell divisions, encodes a putative seven-transmembrane protein similar to the *Drosophila* frizzled protein. *Genes Dev.* **10**, 2189-2197.

Segall, J. E. (1993). Polarization of yeast cells in spatial gradients of alpha mating factor. *Proc. Natl. Acad. Sci. USA* **90**, 8332-8336.

Serafini, T., Kennedy, T. E., Galko, M. J., Mirzayan, C., Jessell, T. M. and Tessier-Lavigne, M. (1994). The netrins define a family of axon outgrowth-promoting proteins homologous to *C. elegans* UNC-6. *Cell* **78**, 409-424.

Steven, R., Kubiseski, T. J., Zheng, H., Kulkarni, S., Mancillas, J., Ruiz, M. A., Hogue, C. W., Pawson, T. and Culotti, J. (1998). UNC-73 activates the Rac GTPase and is required for cell and growth cone migrations in *C. elegans*. *Cell* **92**, 785-795.

Sulston, J., Du, Z., Thomas, K., Wilson, R., Hillier, L., Staden, R., Halloran, N., Green, P., Thierry, M. J., Qiu, L. et al. (1992). The *C. elegans* genome sequencing project: a beginning. *Nature* **356**, 37-41.

Sulston, J. and Hodgkin, J. (1988). Methods. In *The Nematode* Caenorhabditis elegans. (ed. W. B. Wood), pp. 587-605, New York: Cold Spring Harbor Laboratory.

Sulston, J. and Horvitz, H. (1977). Post-embryonic cell lineages of the nematode, *C elegans*. *Dev. Biol.* **56**, 110-156.

Tomic, M., Sunjevaric, I., Savtchenko, E. S. and Blumenberg, M. (1990). A rapid and simple method for introducing specific mutations into any position of DNA leaving all other positions unaltered. *Nucleic Acids Res.* **18**, 1656.

Wadsworth, W. G., Bhatt, H. and Hedgecock, E. M. (1996). Neuroglia and pioneer neurons express UNC-6 to provide global and local netrin cues for guiding migrations in *C. elegans*. *Neuron* **16**, 35-46.

Way, J. C., Run, J. Q. and Wang, A. Y. (1992). Regulation of anterior cell-specific mec-3 expression during asymmetric cell division in *C. elegans*. *Dev. Dyn.* **194**, 289-302.

Whangbo, J. and Kenyon, C. (1999). A Wnt signaling system that specifies two patterns of cell migration in *C. elegans*. *Mol. Cell* **4**, 851-858.

Wood, W. B. (1991). Evidence from reversal of handedness in *C. elegans* embryos for early cell interactions determining cell fates. *Nature* **349**, 536-538.

Zipkin, I. D., Kindt, R. M. and Kenyon, C. J. (1997). Role of a new Rho family member in cell migration and axon guidance in *C. elegans*. *Cell* **90**, 883-894.